

## Some characteristics of $\text{Al}_2\text{O}_3$ - and $\text{CaO}$ -modified $\text{LaFeO}_3$ -based cathode materials for solid oxide fuel cells

Danja Kuščer, Marko Hrovat, Janez Holc, Slavko Bernik, Drago Kolar

*Jožef Stefan Institute, University of Ljubljana, Jamova 39, 61000 Ljubljana, Slovenia*

### Abstract

$\text{Al}_2\text{O}_3$ - and  $\text{CaO}$ -modified  $\text{LaFeO}_3$  were tested as possible solid oxide fuel cell (SOFC) cathode materials. Their electrical and structural characteristics were studied. In the  $\text{La}(\text{Fe}_{1-x}\text{Al}_x)\text{O}_3$  system, specific resistivities increase with increasing concentration of  $\text{Al}_2\text{O}_3$ . The sintered materials are porous and the average grain diameters decrease with increasing  $\text{Al}_2\text{O}_3$  content. In the  $\text{La}_{1-x}\text{Ca}_x\text{FeO}_3$  system, a new single phase, iso-structural with  $\text{LaFeO}_3$ , was observed for  $x=0.5$ . The room temperature resistivities of  $\text{La}_{1-x}\text{Ca}_x\text{FeO}_3$  decrease with increasing values of  $x$ , up to  $x=0.5$ . The resistivity of  $\text{La}_{0.5}\text{Ca}_{0.5}\text{FeO}_3$  is more than four orders of magnitude lower than the resistivity of  $\text{LaFeO}_3$ .

**Keywords:** Solid oxide fuel cells; Perovskites; Ferrites; Conductivity; Microstructure

### 1. Introduction

High-temperature fuel cells with a solid oxide electrolyte (SOFC) work at temperatures around 1000 °C. The solid electrolyte in SOFCs is usually yttria stabilised cubic zirconia (YSZ). The oxygen accepts electrons at the cathode and moves as an ion through the dense  $\text{ZrO}_2$  ceramic. At the anode, ions combine with fuel and release electrons. The advantage of high-temperature SOFCs for production of electrical energy is their high efficiency of 50 to 60%, while some estimates are even to a yield of 70 to 80%. Also, nitrogen oxides are not produced and the amount of  $\text{CO}_2$  released per kWh, due to the high efficiency, is around 50% less than for power sources based on combustion [1–6]. The fuel may be  $\text{H}_2$ , a  $\text{H}_2/\text{CO}$  mixture, or hydrocarbons because the high temperature of operation makes the internal in situ reforming of hydrocarbons with water vapour [7] possible. An extensive and comprehensive review of materials for SOFC is presented in Ref. [8].

For the typical 'working' conditions of the SOFC, the open-circuit voltage (OCV) is around 1 V. However, the operating voltage is lower due to ohmic and polarisation losses at the electrodes. The electrode polarisation losses, related to irreversibilities in the electrochemical processes, are reduced if the electrode material possesses both ionic and electronic conductivities. If the material is an electronic conductor only, the electrochemical reactions can occur solely at the three-phase boundary of, e.g. the cathode, the air (gas

phase) and the electrolyte [9]. If the cathode material possesses a mixed-type conductivity, the reduction of oxygen can occur on the entire surface of the electrode. Also, the thermal expansion coefficients (TECs) of electrode materials must be close to that of YSZ to prevent cracking or delamination of SOFC components either during high temperature operation or heating/cooling cycles.

At present, semiconducting oxides (perovskites), based on  $\text{LaMnO}_3$  or  $\text{LaCoO}_3$  doped with  $\text{SrO}$  and  $\text{CaO}$ , are most often used as the cathode materials. Both have some advantages and some drawbacks. The TEC of  $\text{LaMnO}_3$ -based materials is close to that of YSZ ( $10.5 \times 10^{-6}/\text{K}$ ), but its ionic conductivity is very low. On the other hand, the electronic and ionic conductivities of  $\text{LaCoO}_3$  are high, but its TEC is much higher than that of the solid electrolyte.

Therefore, many alternative cathode materials with mixed conductivities are being investigated for possible use in SOFCs. One of them is  $\text{LaFeO}_3$ , which possesses mixed, i.e. electronic and ionic, conductivity [10] and is therefore a good candidate for the SOFC cathode. The specific resistivity of  $\text{LaFeO}_3$  is around two orders of magnitude higher than that of  $\text{LaMnO}_3$  [11] but it can be decreased by doping with alkaline earth oxides [12]. It is interesting to note that, while many papers describe the influence of  $\text{SrO}$  doping on the characteristics of lanthanum ferrite, there are, at least to the authors' knowledge, no data in the open literature on the influence of  $\text{CaO}$  doping on the electrical parameters of  $\text{LaFeO}_3$ .

A range of solid solubilities exists between  $\text{LaFeO}_3$  and  $\text{LaAlO}_3$  which enables some 'tailoring' of material characteristics [13]. Undoped  $\text{LaAlO}_3$  is a dielectric, while doped  $\text{LaAlO}_3$  becomes a mixed conductor [14]. The partial exchange of iron oxide with alumina in  $\text{LaFeO}_3$  perovskite also decreases the rate of reaction between the YSZ solid electrolyte and the lanthanum perovskite-based cathode [11,15]. It is known that practically all lanthanum perovskites used for SOFCs, with the possible exception of chromites [16], react with zirconia forming undesirable  $\text{La}_2\text{Zr}_2\text{O}_7$  at the interface. The specific electrical resistivity of  $\text{La}_2\text{Zr}_2\text{O}_7$  is more than two orders of magnitude higher than that of YSZ leading to increased cell losses due to increased internal resistivity and therefore decreases in its yield [8,17–21].

In this work an evaluation of the electrical and microstructural characteristics of  $(\text{La}_{1-x}\text{Ca}_x)\text{FeO}_3$  (for  $x$  between 0 and 1) and  $\text{La}(\text{Fe}_{1-x}\text{Al}_x)\text{O}_3$  (for  $x$  between 0 and 0.96) based materials is described. It should be mentioned that alumina-rich perovskites, i.e.  $x=0.94$ , are not of interest for SOFC cathodes due to their high specific resistivities, and are included to cover the entire  $\text{Al}_2\text{O}_3$  concentration range.

## 2. Experimental

For experimental work,  $\text{La}(\text{OH})_3$  (Ventron, 99.9%),  $\text{Fe}_2\text{O}_3$  (Alfa, 99.9%),  $\text{Al}_2\text{O}_3$  (Alcoa, A-16, +99%), and  $\text{CaCO}_3$  (Merck, +99%) were used. The samples were mixed in isopropyl alcohol, pressed into pellets, pre-fired at 1000 °C, and fired twice at 1200 °C for 10 h with intermediate grinding. During firing pellets were placed on platinum foils. The composition of the samples were  $\text{La}_{1-x}\text{Ca}_x\text{FeO}_3$  with  $x=0, 0.1, 0.3, 0.5, 0.75$ , and 1 and  $\text{La}(\text{Fe}_{1-x}\text{Al}_x)\text{O}_3$  with  $x=0, 0.2, 0.4, 0.5, 0.8$ , and 0.96. The chosen compositions are shown schematically in Figs. 1 and 2 for  $\text{La}(\text{Fe}_{1-x}\text{Al}_x)\text{O}_3$  and  $\text{La}_{1-x}\text{Ca}_x\text{FeO}_3$ , respectively. The binary compound  $\text{CaFe}_4\text{O}_9$  is stable only in a narrow temperature range between 1155 and 1276 °C [22]. Fired materials were investigated by X-ray powder diffraction (XRD) analysis. Microstructures of samples were observed by scanning electron microscopy (SEM) and analysed by energy dispersive X-ray microanalysis (EDS). Electrical d.c. resistance was measured by the

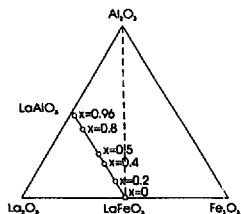


Fig. 1. Chosen compositions in the  $\text{La}(\text{Fe}_{1-x}\text{Al}_x)\text{O}_3$  system.

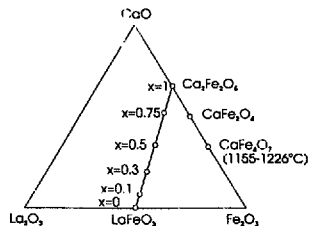


Fig. 2. Chosen compositions in the  $\text{La}_{1-x}\text{Ca}_x\text{FeO}_3$  system.

four-point method in the 20–920 °C temperature range in air. Unfired Pt electrodes (Demetron MR014) were printed as contacts on the samples and fired for 30 min at 1000 °C.

## 3. Results and discussion

### 3.1. $\text{La}(\text{Fe}_{1-x}\text{Al}_x)\text{O}_3$

XRD spectra of materials with the nominal composition  $\text{La}(\text{Fe}_{1-x}\text{Al}_x)\text{O}_3$  are shown in Fig. 3. Samples with  $x=0$  ( $\text{LaFeO}_3$ ) and  $x=0.4$  are single-phase solid solutions of  $\text{Al}_2\text{O}_3$  in  $\text{LaFeO}_3$ , while the sample with  $x=0.5$ , i.e. with nominal composition  $\text{La}(\text{Fe}_{0.5}\text{Al}_{0.5})\text{O}_3$  is a two-phase mixture of a solid solution of  $\text{Al}_2\text{O}_3$  in  $\text{LaFeO}_3$  and a solid solution of  $\text{Fe}_2\text{O}_3$  in  $\text{LaAlO}_3$ . The X-ray spectrum of  $\text{LaAlO}_3$  ( $x=1$ ) is also shown for comparison.

Specific resistivities of  $\text{La}(\text{Fe}_{1-x}\text{Al}_x)\text{O}_3$  at room temperature and at 920 °C are summarised in Table 1.

Specific resistivities increase with increasing concentration of  $\text{Al}_2\text{O}_3$ . Resistivities of samples with  $x=0, 0.2$  and 0.4 are relatively close together while for higher concentrations of alumina the increase in resistivity is more pronounced. This

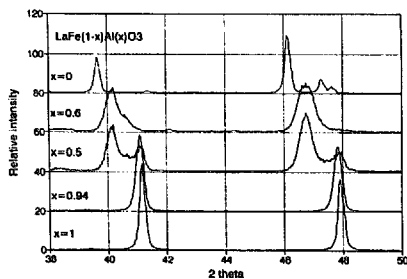


Fig. 3. X-ray spectra of materials with nominal composition  $\text{La}(\text{Fe}_{1-x}\text{Al}_x)\text{O}_3$ . The sample with  $x=0.5$ , i.e. with a nominal composition  $\text{La}(\text{Fe}_{0.5}\text{Al}_{0.5})\text{O}_3$  is a two-phase mixture of a solid solution of  $\text{Al}_2\text{O}_3$  in  $\text{LaFeO}_3$  and solid solution of  $\text{Fe}_2\text{O}_3$  in  $\text{LaAlO}_3$ .

**Table 1**  
Specific resistivities of materials with nominal compositions  $\text{La}(\text{Fe}_{1-x}\text{Al}_x)\text{O}_3$  at room temperature and at 920 °C

$\text{La}(\text{Fe}_{1-x}\text{Al}_x)\text{O}_3$	Specific resistivity at room temperature ( $\Omega \text{ m}$ )	Specific resistivity at 920 °C ( $\Omega \text{ m}$ )
$x = 0$	6700	0.029
$x = 0.2$	15000	0.10
$x = 0.4$	25000	0.16
$x = 0.5$	160000	0.95
$x = 0.94$	$> 100 \times 10^6$	63

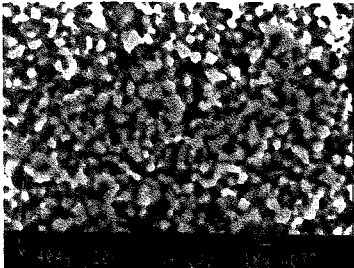


Fig. 4. The microstructure of  $\text{La}(\text{Fe}_{0.8}\text{Al}_{0.2})\text{O}_3$  fired 60 h at 1200 °C

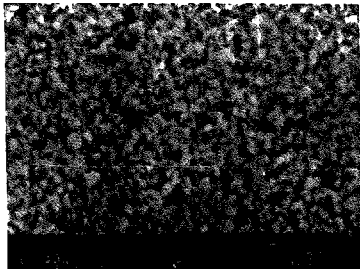


Fig. 5. The microstructure of  $\text{La}(\text{Fe}_{0.6}\text{Al}_{0.4})\text{O}_3$  fired 60 h at 1200 °C.

is presumably due to the solid solution limit of  $\text{Al}_2\text{O}_3$  in  $\text{LaFeO}_3$  [13].

The microstructures of  $\text{La}(\text{Fe}_{1-x}\text{Al}_x)\text{O}_3$  samples fired for 60 h at 1200 °C are shown in Fig. 4 ( $x = 0.2$ ) and Fig. 5 ( $x = 0.4$ ). The microstructures are porous and average grain diameters decrease with increasing  $\text{Al}_2\text{O}_3$  content.

### 3.2. $(\text{La}_{1-x}\text{Ca}_x)\text{FeO}_3$

X-ray spectra of materials with the nominal composition  $\text{La}_{1-x}\text{Ca}_x\text{FeO}_3$  ( $x = 0, 0.1, 0.3, 0.5, 0.75, \text{ and } 1$ ) are shown

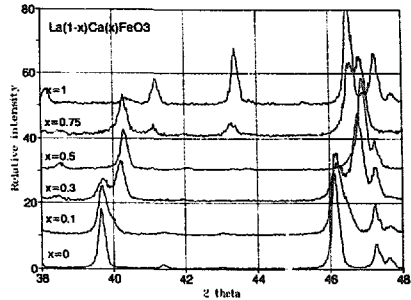


Fig. 6. X-ray spectra of materials with the nominal composition  $\text{La}_{1-x}\text{Ca}_x\text{FeO}_3$ . For  $x = 0.5$  a new single phase, isostructural with  $\text{LaFeO}_3$ , was observed.

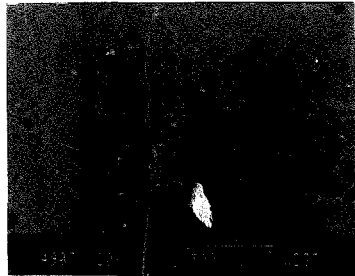


Fig. 7. The microstructure of material with nominal composition  $\text{La}_{0.7}\text{Ca}_{0.3}\text{FeO}_3$ . Dark gray inclusions represent a calcium-rich phase.

in Fig. 6. For  $x = 0.1$  only peaks of the solid solution of  $\text{CaO}$  in  $\text{LaFeO}_3$  were observed. At  $x = 0.3$  two phases were noticed while for  $x = 0.5$  only a new single phase was observed. This phase is iso-structural with  $\text{LaFeO}_3$ . The sample with  $x = 0.75$  is a mixture of  $\text{La}_{0.5}\text{Ca}_{0.5}\text{FeO}_3$  and  $\text{Ca}_2\text{Fe}_2\text{O}_7$ .

The microstructures of samples with  $x = 0.3$  and  $0.5$  are shown in Figs. 7 and 8, respectively. A microphotograph of the material with the nominal composition  $\text{La}_{0.7}\text{Ca}_{0.3}\text{FeO}_3$  shows inclusions of a darker, calcium-rich phase in a lighter matrix while material with  $x = 0.5$  is single phase.

Specific resistivities of  $\text{La}_{1-x}\text{Ca}_x\text{FeO}_3$  at room temperature and at 920 °C are summarised in Table 2.

The room temperature resistivities of  $\text{La}_{1-x}\text{Ca}_x\text{FeO}_3$  decrease with increasing values of  $x$  to  $x = 0.5$  and then increase with further increase in  $x$ . The resistivity of the  $\text{La}_{0.5}\text{Ca}_{0.5}\text{FeO}_3$  is more than four orders of magnitude lower than the resistivity of  $\text{LaFeO}_3$ , and at temperatures over 100 °C (specific resistivity around 0.05  $\Omega \text{ m}$ ) is practically independent of the temperature. The independence of resis-

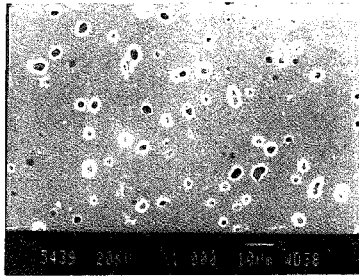


Fig. 8. The microstructure of material with nominal composition  $\text{La}_{0.5}\text{Ca}_{0.5}\text{FeO}_x$ .

Table 2  
Specific resistivities of materials with nominal compositions  $\text{La}_{1-x}\text{Ca}_x\text{FeO}_x$  at room temperature and at 920 °C

$\text{La}_{1-x}\text{Ca}_x\text{FeO}_x$	Specific resistivity at room temperature ( $\Omega \text{ m}$ )	Specific resistivity at 920 °C ( $\Omega \text{ m}$ )
$x=0$	6700	0.029
$x=0.1$	16.6	0.074
$x=0.3$	3.50	0.026
$x=0.5$	0.26	0.038
$x=0.75$	7.75	0.125
$x=1$	110000	1.085

tivity versus temperature, i.e. the low resistivity over the entire temperature range, could be important for the next generation of SOFCs aiming at lower working temperatures around or under 850 °C.

#### 4. Conclusions

$\text{Al}_2\text{O}_3$ - and  $\text{CaO}$ -modified  $\text{LaFeO}_3$  were tested as possible solid oxide fuel cell (SOFC) cathode materials. Materials with nominal compositions  $\text{La}(\text{Fe}_{1-x}\text{Al}_x)\text{O}_3$  ( $x=0$  to  $x=0.94$ ) and  $\text{La}_{1-x}\text{Ca}_x\text{FeO}_{3-y}$  ( $x=0$  to  $x=1$ ) were synthesised. The materials were studied by XRD analysis, SEM and EDS microanalysis. D.c. resistivities were measured as a function of temperature.

In the  $\text{La}(\text{Fe}_{1-x}\text{Al}_x)\text{O}_3$  system, specific resistivities increase with increasing concentration of  $\text{Al}_2\text{O}_3$ . Resistivities of samples with  $x=0.2$  and  $0.4$  are relatively close together while for higher concentrations of alumina the increase in resistivity is more pronounced. This is presumably due to the solid solution limit of  $\text{Al}_2\text{O}_3$  in  $\text{LaFeO}_3$ , as shown also by the

X-ray spectra. The sintered materials are porous and average grain diameters decrease with increasing  $\text{Al}_2\text{O}_3$  content.

In the  $\text{La}_{1-x}\text{Ca}_x\text{FeO}_3$  system a new single phase, iso-structural with  $\text{LaFeO}_3$ , was observed for  $x=0.5$ . The room temperature resistivities of  $\text{La}_{1-x}\text{Ca}_x\text{FeO}_3$  decrease with increasing values of  $x$  up to  $x=0.5$ . The resistivity of  $\text{La}_{0.5}\text{Ca}_{0.5}\text{FeO}_3$  is more than four orders of magnitude lower than the resistivity of  $\text{LaFeO}_3$  and at temperatures over 100 °C is practically independent of temperature.

#### Acknowledgements

Part of this work ( $\text{La}(\text{Fe}_{1-x}\text{Al}_x)\text{O}_3$ -based materials) was performed within the project 'New SOFC Materials and Technology, J0U2-CT92-0063'. The authors would like to express their thanks to Dr Tomaž Kosmač for helpful discussions. The financial support of the Ministry of Science and Technology of Slovenia is gratefully acknowledged.

#### References

- [1] N.Q. Minh, *Chemtech.*, (2) (1991) 120–126.
- [2] K. Kendall, *Ceram. Bull.*, 70 (1991) 1159–1160.
- [3] F. Gross, in F. Grosz, P. Zegers, S.C. Singhal and O. Yamamoto (eds.), *Solid oxide fuel cells' R&D in Europe, Proc. 2nd Int. Symp. Solid Oxide Fuel Cells*, Commission of the European Communities, Athens, 1991, pp. 7–23.
- [4] M. Mogensen and N. Christiansen, *Europhys. News*, 24 (1993) 7–9.
- [5] H. Tagawa, in S.C. Singhal and H. Iwahara (eds.), *Status of SOFC development in Japan, Proc. 3rd Int. Symp. Solid Oxide Fuel Cells, Honolulu, HI, USA, 1993*, The Electrochemical Society, Pennington, NJ, USA, pp. 6–15.
- [6] S. Kartha and P. Grimes, *Phys. Today*, 47 (11) (1994) 54–61.
- [7] K. Ledjeff, T. Rohrbach and G. Schaunberg, *Phys. Today*, 47 (11) 323–333.
- [8] N.Q. Minh, *J. Am. Ceram. Soc.*, 76 (1993) 563–588.
- [9] J. Mizusaki, H. Tagawa, T. Saito, K. Kamitani, T. Yamamura, K. Hirano, S. Ehara, T. Takagi, T. Hikita, M. Ippommatsu, S. Nakagawa and K. Hashimoto, in S.C. Singhal and H. Iwahara (eds.), *Preparation of nickel pattern electrodes on YSZ and their electrochemical properties in  $\text{H}_2$ - $\text{H}_2\text{O}$  atmospheres, Proc. 3rd Int. Symp. Solid Oxide Fuel Cells, Honolulu, HI, USA, 1993*, The Electrochemical Society, Pennington, NJ, USA, pp. 533–541.
- [10] L.W. Tai, M.M. Nasrallah and H.U. Anderson, in S.C. Singhal and H. Iwahara (eds.), *( $\text{La}_{1-x}\text{Sr}_x$ )( $\text{Co}_{1-y}\text{Fe}_y$ ) $\text{O}_3$ , a potential cathode for intermediate temperature SOFC applications, Proc. 3rd Int. Symp. on Solid Oxide Fuel Cells, Honolulu, HI, USA, 1993*, The Electrochemical Society, Pennington, NJ, USA, pp. 241–251.
- [11] D. Kuščer, M. Hrovat, J. Holc, S. Bernik and D. Koiar, *Thick film  $\text{LaFeO}_3$  based cathodes for SOFC: electrical characteristics and interactions with YSZ solid electrolyte, Proc. 10th European Microelectronics Conf. ISHM-Europe 95, Copenhagen, 1995*, pp. 356–361.
- [12] J. Mizusaki, T. Sasamoto, W.R. Cannon and H.K. Bowen, *J. Am. Ceram. Soc.*, 66 (1983) 247–252.
- [13] M. Hrovat, J. Holc, D. Kuščer, Z. Samardžija and S. Bernik, *J. Mater. Sci. Lett.*, 14 (1995) 265–267.

- [14] H. Matsuda, T. Ishihara, Y. Mizuhara and Y. Takita, in S.C. Singhal and H. Iwahara (eds.), Oxygen ion conductivity of doped  $\text{LaAlO}_3$  perovskite oxide, *Proc. 3rd Int. Symp. Solid Oxide Fuel Cells, Honolulu, HI, USA, 1993*, The Electrochemical Society, Pennington, NJ, USA, pp. 129–136.
- [15] D. Kuščer, M. Hrovat, J. Holc, S. Bernik and D. Kolar, Electrical and microstructural characterisation of  $\text{Al}_2\text{O}_3$  doped  $\text{LaMnO}_3$ , *J. Mater. Sci. Lett.*, 14 (1995) 1684–1687.
- [16] M. Hrovat, S. Bernik, J. Holc, D. Kolar and B. Dacar, Preliminary data on subsolidus phase equilibria in the  $\text{La}_2\text{O}_3$ - $\text{Cr}_2\text{O}_3$ - $\text{Y}_2\text{O}_3$  and  $\text{La}_2\text{O}_3$ - $\text{Cr}_2\text{O}_3$ - $\text{ZrO}_2$  systems, *J. Mater. Sci. Lett.*, 14 (1995) 1684–1687.
- [17] H. Taimatsu, K. Wada and H. Kaneko, *J. Am. Ceram. Soc.*, 75 (1992) 401–405.
- [18] J.A.M. van Roesmalen and E.H.P. Cordfunke, *Solid State Ionics*, 52 (1992) 303–312.
- [19] J.A. Labrincha, J.R. Frade and F.M.B. Marques, *J. Mater. Sci.*, 28 (1993) 3809–3815.
- [20] J. Stochmiol, E. Syskakis and A. Naoumidis, *J. Am. Ceram. Soc.*, 78 (1995) 929–932.
- [21] D. Kuščer, J. Holc, M. Hrovat, S. Bernik, Z. Samardžija and D. Kolar, *Solid State Ionics*, 78 (1995) 79–85.
- [22] E.M. Levin, C.R. Robbins and H.F. McMurdie (eds.), *System CaO-Fe<sub>2</sub>O<sub>3</sub> in air, Phase Diagrams for Ceramists*, Vol. 1, The American Ceramic Society, 1964, p. 49, Fig. 43. (After B. Phillips, A. Muan, *J. Am. Cer. Soc.*, 42 (11) (1958).)